Asian Journal of Chemistry; Vol. 36, No. 7 (2024), 1571-1578

ASIAN JOURNAL OF CHEMISTRY

https://doi.org/10.14233/ajchem.2024.31456

Selective Sensing and Determination of Cu^{2+} Ions in Environmental Samples with Newly Prepared Quinoline based Chemosensors and Confirmation of Results using DFT Molecular Modelling

G.O. OBAIAH[1], M.A. ABDULZAHRA[2], A. TEWARI[3], M.S. PATEL[4], V.S. TALISMANOV[5], N.K. SHARMA[6], S. SEHLANGIA[7,*] and M.S. THAKARE[8,*]

[1]Department of Chemistry, Karnataka State Open University, Mukhtagangotri, Mysuru-570006, India
[2]Department of Pharmacy, Al-Amal College for Specialized Medical Sciences, Karbala-56001, Iraq
[3]Department of Basic Science and Humanities, Pranveer Singh Institutue of Technology, Bhauti, Kanpur-209305, India
[4]Mohammed Al-Mana College for Medical Sciences, Dammam, Kingdom of Saudi Arabia
[5]Department of Chemistry, Moscow Institute of Physics and Technology, Dolgoprudny, Moscow Region, 141701, Russian Federation
[6]Department of Chemistry, Government P.G. College, Bundi-323001, India
[7]Department of Chemistry, School of Basic Sciences, Indian Institute of Technology Mandi, Kamand-175005, India
[8]Department of Chemistry, Pratap College (Autonomous), Amalner-425401, India

*Corresponding authors: E-mail: sumanyadav1708@gmail.com; milindthakare@pec.ac.in

Received: 29 February 2024; *Accepted*: 9 May 2024; *Published online*: 29 June 2024; AJC-21676

An efficient turn-off-fluorescence chemosensing method has been developed to detect Cu^{2+} ions in a variety of samples. Two new quinoline-based chemosensors (**QC1** and **QC2**) have been prepared under the condensation reaction of 8-quinolinecarboxylic acid with derivatives of L-valine. The synthesized chemosensors were characterized by spectroscopic techniques such as ^{1}H NMR, UV, IR, HRMS and CHNS. The HOMO-LUMO orbitals and energy-minimized structures of the chemosensors were developed. The interaction of metal ions with chemosensors and stable structures of complexes were investigated using DFT. The photoluminescence analysis of both chemosensors (**QC1** and **QC2**) showed the fluorescence emission wavelengths on 495 and 512 nm, respectively, for **QC1** and **QC2**. The change in fluorescence emission wavelengths depends on the electronic effects of the substituents on the quinoline ring. The chemosensors showed a high sensitivity for Cu ions; thus, the detection was exhibited in nanomolar levels. The chemosensing studies were performed in the presence of different metal ions and samples taken from other sources.

Keywords: L-Valine, Quinoline derivatives, Fluorescent probes, Chemosensor, Environmental samples.

INTRODUCTION

Copper is the third-most prevalent transition element in the body; it is crucial for many physiological processes, including the manufacture of haemoglobin, the formation of bones, the synthesis of dopamine, the regulation of nerve activity, the expression of genes and the improvement of protein structure and function [1-4]. However, Cu^{2+} is highly hazardous to living things when overloaded. For instance, excessive accumulation in humans results in several illnesses, such as coronary heart disease, metabolic and genetic problems, obesity, diabetes and Wilson's disease [5,6]. Commonly, human blood typically has an average quantity of Cu^{2+} between 15.7-23.6 μM [7]. However, Cu^{2+} pollution has skyrocketed globally due to the extensive use of copper in water pipelines, industry, agriculture and household appliances. As a result, quick, practical and trustworthy analytical techniques must be developed to identify copper both qualitatively and quantitatively, especially in biological samples and drinking water. Thus, more advanced technologies and methods are required for the qualitative and quantitative detection of copper.

Recently, the growing need for effective and adaptable luminous systems for materials, biological and chemical applications has led to an active research area in developing novel luminescent molecules [8-14]. Among the different chromophores used in creating luminous materials, substituted quinoline has drawn the most interest because of its distinct coordination and photophysical characteristics [15]. Tris(hydroxyl-8-

quinolinato)aluminium(III), for instance, is one of the most influential metal complexes for OLED applications that have been explored to date. This is due to quinoline's exceptional optical and chelating characteristics [16]. Quinolines are naturally occurring fused rings of aromatic molecules belonging to a heterocyclic class. The quinoline and its derivatives have been used vastly in industrial and medicinal applications [9,10,12]. Quinoline derivatives are primarily used in treating bacterial infection, inflammation, cancer, malaria, fungal infection and leishmaniasis. Quinoline derivatives are used to prepare sensors, anti-foaming agents in refineries, dyes, paint, corrosion inhibitors and other petrochemical and chromatographic applications [1-3,16-19]. Qulinolines, due to the aromatic system of fused rings, show excellent fluorophores and luminescent properties. Thus, it has gained massive attention in preparing fluorescence and luminescent chemosensors. The chemosensors based on quinolones show great binding capacity with different analytes due to the presence of the heteroatom (nitrogen atom; act as electro-donor) in the structure and offer highly sensitive detections of analytes in different situations with remarkable sensitivity. Until now, various quinoline-based fluorophoric chemosensors have been developed by derivatizing quinoline at second and eighth positions, for example, the styryl substituted 8-hydroxyquinoline derivatives [9,10]. Quinoline-based chemosensors have been used to detect a variety of metal cations in different samples from chemical, environmental, clinical and biological samples, such as zinc, iron, cobalt, copper, calcium, magnesium, *etc.* [1,12] and have been used in other applications such as chromatographic detections [13,17-19].

Herein, we report the synthesis of two novel quinoline-based chemosensors (**QC1** and **QC2**), by introducing L-valine into quinoline. Amino acid as a substituent allows electronic fine-tuning and controls of the overall properties of the chemosensors by raising the electron withdrawing or donating substituents on the quinoline. The synthesized chemosensors are used to develop a fluorophores chemosensing method for different metal ions from environmental samples. The computational calculations were also performed to optimize HOMO-LUMO and energy gap, stable structure and metal complex. The sensitivity and selectivity toward the copper ion were also calculated.

EXPERIMENTAL

L-Valine, oxalyl chloride, hexyl bromide, bromomethyl pyridine and 8-quinoline carboxylic acid were purchased from Sigma-Aldrich. The industrial and river water samples were collected from nearby locations. The solvents acetone, ethyl acetate, dichloromethane, chloroform, methanol) and other reagents used in current study were purchased from Avra Chemicals (India).

Characterization: The UV-2450 spectrophotometer (Shimadzu), fluorescence spectrometer (Agilent), FT-IR spectrophotometer (Agilent), NMR instrument (Jeol 500 MHz), HR-MS (Bruker HD) and elemental analyzer were used to characterized synthesis products.

Synthesis of derivatives of L-valine (V1 and V2): L-Valine (5 mmol) and solid K_2CO_3 (20 mmol) were added to 30 mL dry THF and heated to dissolve. In this solution, hexyl bromide solution (5 mmol) in 15 mL dry THF was added slowly. This reaction mixture was then allowed to stir for 20 h under refluxing. The progress of the reaction was monitored using TLC [20]. Upon completion, the reaction solution was passed through filter paper and the solid residue was removed. The filtrate was then concentrated and dried under reduced pressure. The column chromatography was performed to obtain the desired purified product (**V1**) [21,22]. Similarly, under the substitution reaction another derivative (**V2**) of L-valine was prepared. The chemical structures of the **V1** and **V2** (derivatives of L-valine) are given in Fig. 1.

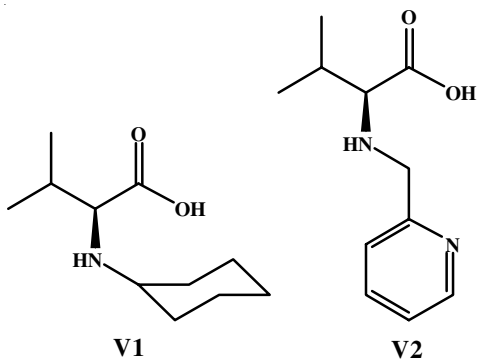

Fig. 1. Structures of derivatives of L-valine prepared under substitution reaction with hexyl bromide (**V1**) and bromomethyl pyridine (**V2**)

V1: Off-white solid; yield: 53%; ^{1}H NMR (500 MHz, $CDCl_3$-d_6) δ ppm: 0.92-0.99 (6H, dd), 1.34-1.46 (5H, m), 1.52-1.69 (3H, m), 1.74-1.82 (2H, m), 2.06-2.11 (1H, m), 2.68-2.77 (1H, m), 3.06-3.11 (1H, m) and 4.08-4.14 (1H, m). HRMS [$C_{11}H_{21}NO_2$]: 199.17 ($M+H^+$); Anal. calcd. (found) % for $C_{11}H_{21}NO_2$: C, 66.29 (65.89); H, 10.62 (9.92); N, 7.03 (7.58).

V2: Pale-yellow solid; yield: 67%; ^{1}H NMR (500 MHz, $CDCl_3$-d_6) δ ppm: 0.92-0.98 (6H, dd), 2.07-2.14 (1H, m), 3.38-3.42 (1H, m), 4.02-4.06 (1H, dd), 4.13-4.18 (1H, dd), 4.72-4.76 (1H, m), 7.26-7.28 (1H, d), 7.46-7.49 (1H, m), 7.61-7.64 (1H, t), 8.51-8.52 (1H, dd). HRMS [$C_{11}H_{16}N_2O_2$]: 208.18 ($M+H^+$); Anal. calcd. (found) % for $C_{11}H_{16}N_2O_2$: C, 63.44 (64.16); H, 7.74 (7.25); N, 13.45 (12.86).

Synthesis of 8-quinolinecarboxylic acid based chemosensors (QC1 and QC2): In the presence of a catalytic amount of pyridine, the carboxylic group of 8-quinolinecarboxylic acid was activated by oxalyl chloride [20-25]. The acid chloride group was then converted to amide through a substitution reaction with the synthesized derivatives of L-valine (**V1** and **V2**), as shown in **Scheme-I** [22,26].

QC1: Pale yellow solid; yield: 97%; ^{1}H NMR (500 MHz, $CDCl_3$-d_6) δ ppm: 0.92-0.99 (dd, 6H), 1.34-1.46 (m, 5H), 1.52-1.69 (m, 3H), 1.74-1.82 (m, 2H), 2.06-2.11 (m, 1H), 2.68-2.77 (m, 1H), 3.06-3.11 (m, 1H), 4.08-4.14 (m, 1H), 7.46-7.49 (t, 1H), 7.57-7.59 (m, 1H), 8.08-8.11 (dt, 1H), 8.25-8.27 (dt, 1H), 8.86-8.88 (dd, 1H). HRMS [$C_{21}H_{26}N_2O_3$]: 355.28 ($M+H^+$); Anal. calcd. (found) % for $C_{21}H_{26}N_2O_3$: C, 71.16 (71.84); H, 7.39 (6.67); N, 7.90 (8.34).

QC2: Brownish-yellow solid; yield: 96%; ^{1}H NMR (500 MHz, $CDCl_3$-d_6) δ ppm: 0.92-0.98 (6H, dd), 2.07-2.14 (1H, m), 3.38-3.41 (1H, m), 4.02-4.07 (1H, dd), 4.12-4.17 (1H, dd),

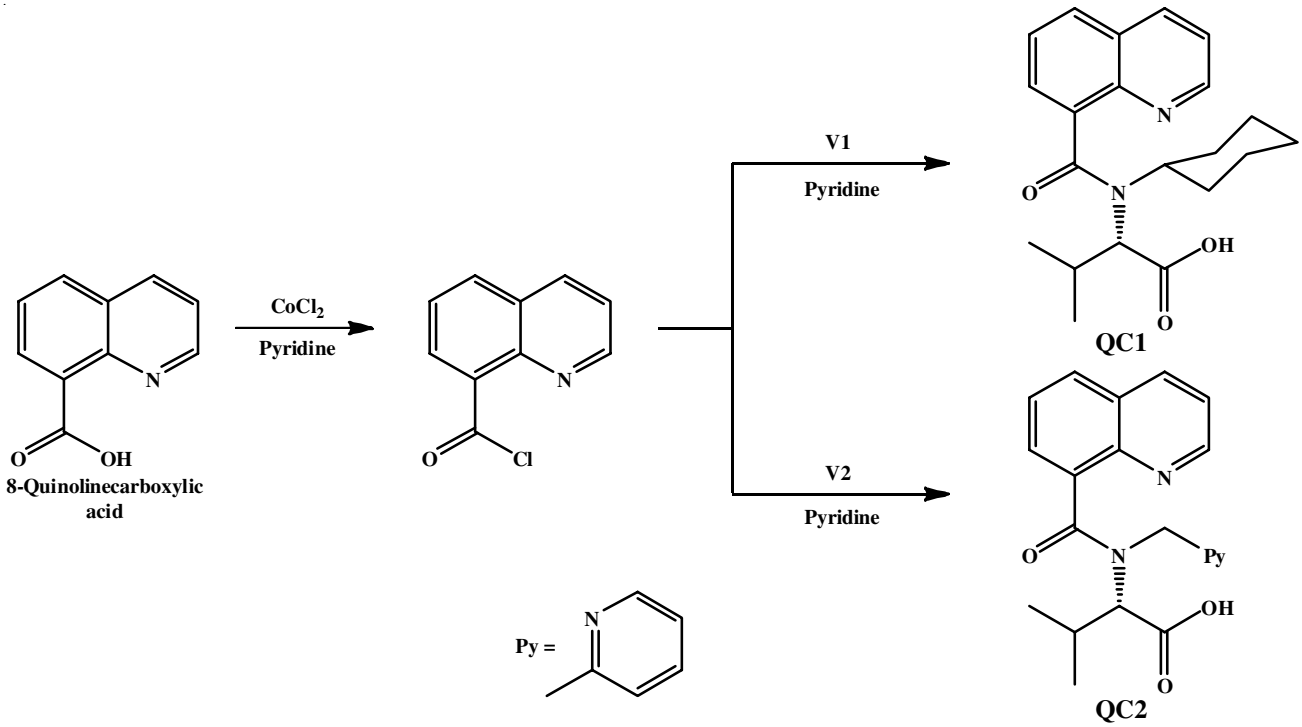

Scheme-I: Synthesis of quinoline-based chemosensors [(i) **QC1** and (ii) **QC2**]

4.73-4.78 (1H, m), 7.25-7.27 (1H, d), 7.47-7.49 (1H, m), 7.61-7.65 (1H, t), 8.51-8.52 (1H, dd), 7.46-7.48 (1H, t), 7.57-7.60 (1H, m), 8.07-8.09 (1H, dt), 8.24-8.27 (1H, dt) and 8.87-8.89 (1H, dd). HRMS [$C_{21}H_{21}N_3O_3$]: 363.21 ($M+H^+$); Anal. calcd. (found) % for $C_{21}H_{21}N_3O_3$: C, 69.41 (70.11); H, 5.82 (6.26); N, 11.56 (11.78).

RESULTS AND DISCUSSION

The L-valine was converted to its substituted derivatives under the substitution reaction, where the bromo group (leaving group) of hexyl bromide or bromomethyl pyridine was substituted with an amino group of L-valine [23] and yields around 68-72% yield. The carboxylic group of 8-quinolinecarboxylic acid, in the presence of chlorinating reagent (oxalyl chloride and pyridine), was converted to acyl chloride under S_N^2 substitution. The chlorinating reagent, oxalyl chloride and catalyst (pyridine), is considered an excellent reagent for the acylation of carboxylic groups [22,23,27] and yields nearly 100% of the desired product. Acyl chloride is very potent toward the nucleophile attack. It gives the easy formation of an ester of the amide bond in the presence of suitable nucleophiles under the substitution reaction and yields a remarkable amount of products [28-30]. Following this, the acyl chloride of 8-quinoline-carboxylic acid and the amino group of L-valines (**V1** or **V2**) were allowed to react in the presence of catalytic amount of pyridine. The reactants were quickly reacted and yielded nearly 100% of the desired chemosensor (**QC1** and **QC2**). The prepared and purified chemosensors were then characterized by spectroscopic methods.

It is well-known that compounds based on quinole have fascinating photoluminescence characteristics [5,31-33]. Thus, in a mixture of methanol and buffer (HEPES) (9.5: 0.5%, v/v), the fluorescence characteristics of **QC1** and **QC2** (5×10^{-5} M) were examined. The maximum fluorescence emissions were observed at 495 and 512 nm for the chemosensors **QC1** and **QC2**, respectively. The fluorescence emission that **QC1** and **QC2** exhibited was in the following order: **QC2** > **QC1**. Since the main difference between the two chemosensors is in the amino acids, it is plausible to conclude that the amino acid's electronic effect substantially influences the chemosensors' fluorescence properties.

Since **QC1** and **QC2** have suitable binding sites, therefore can be examined their chemosensing capacities for several metal ions, including Ag^+, Mn^{2+}, Al^{3+}, Na^+, Cr^{3+}, Ni^{2+}, Pb^{2+}, Fe^{3+}, Cd^{2+}, Hg^{2+}, Zn^{2+} and Cu^{2+}. When present in excess, many of these metal ions are identified as harmful environmental contaminants and can harm health. Except for Cu^{2+}, there were no discernible changes in the fluorescence intensities of **QC1** and **QC2** solutions following the addition of these metal ions. The addition of Cu^{2+} to the **QC1** and **QC2** solutions resulted in a considerable quenching of the fluorescence peaks at 495 and 512 nm, respectively (Fig. 2a-b) shows the fluorescence spectra of **QC1** and **QC2**).

The detection limit (LOD) of the prepared chemosensors (**QC1** and **QC2**) for for Cu^{2+} ions were estimated. The IUPAC guidlines define a standered relationship (*i.e.* LOD = (3.3 × standard deviation)/slope) to calculate the LOD values. The measurements of ten blank samples were taken to calulate the relative standered deviation in current report. The calculated LOD values of **QC1** and **QC2** were 59.27 nM and 40.96 nM, respectively, towards Cu^{2+} [34], Fig. 3a-b respectively. **QC2** had the lowest LOD towards Cu^{2+} than **QC1**.

Using the Benesi-Hildebrand method, the binding constants **of QC1** and **QC2** towards Cu^{2+} were determined to be 0.76 ×

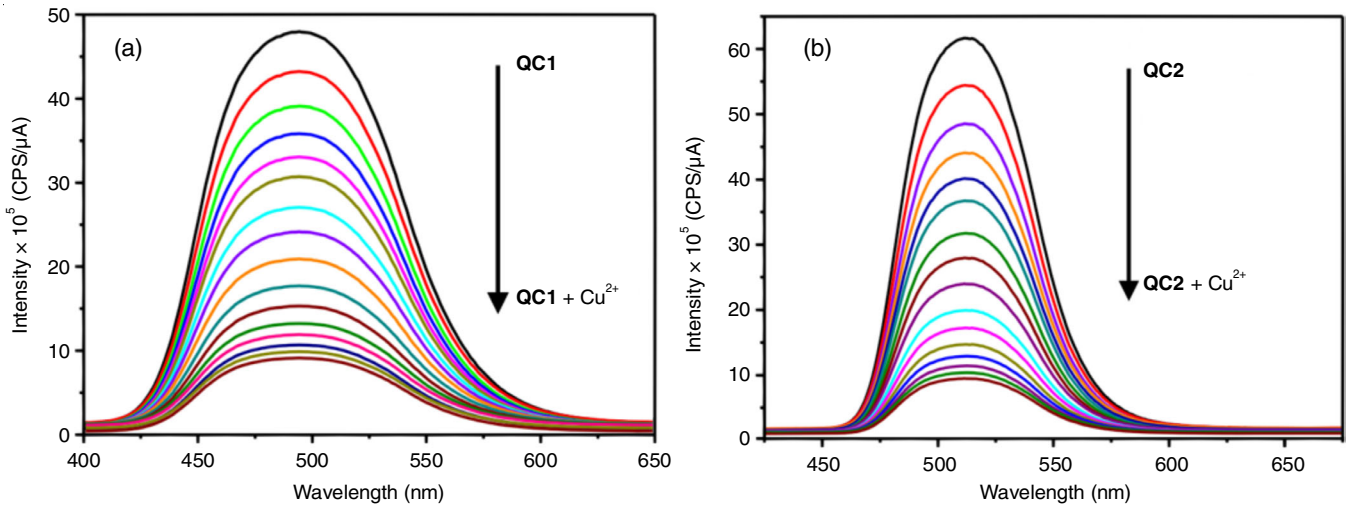

Fig. 2. Fluorescence spectra of **QC1** (a) and **QC2**, (b) (5×10^{-5} M) respectively in MeOH:H_2O (9.5:0.5%,v/v) upon incremental addition of Cu^{2+} ions

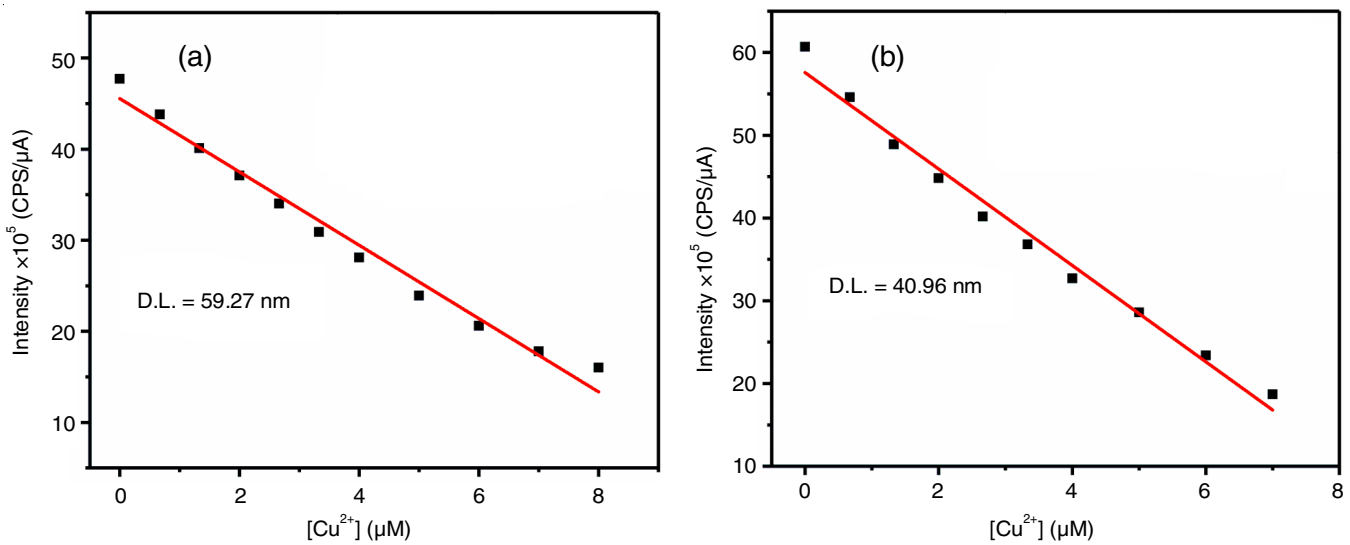

Fig. 3. The limit of detection of **QC1** (a) and **QC2** (b) with Cu^{2+} respectively

10^5 M^{-1} and 0.98×10^5 M^{-1}, respectively (Fig. 4a-b). Moreover, using Stern-Volmer plots, the quenching constants for **QC1** and **QC2** towards Cu^{2+} were determined to be 1.30×10^5 M^{-1} and 1.51×10^5 M^{-1}, respectively. The non-linear characteristics and upward bend of the Stern-Volmer plots in each of these examples (Fig. 5a-b Stern-Volmer plot of **QC1**, as representative) indicate that a combination of dynamic and static quenching is responsible for the quenching of the fluorescence [35].

We performed competing studies with other cations (Ag^+, Mn^{2+}, Al^{3+}, Na^+, Cr^{3+}, Ni^{2+}, Pb^{2+}, Fe^{3+}, Cd^{2+}, Hg^{2+} and Zn^{2+}) present under comparable experimental conditions to evaluate the great selectivity of **QC1** and **QC2** towards Cu^{2+} ions. These investigations showed that other metal cations did not significantly interfere with **QC1** and **QC2**'s ability to detect Cu^{2+} (Fig. 6a-b). Consequently, **QC1** and **QC2** are extremely selective fluorescence chemosensors to identify Cu^{2+}.

Job's plot analysis was performed to verify the stoichiometry and the mechanism of **QC1** and **QC2** interaction with Cu^{2+}. The highest fluorescence intensity for **QC1** and **QC2** was observed at 0.5 mol fraction, indicating a stoichiometry ratio of 1:1, according to the Job's plot [36], the fluctuation of the fluoresence intensity (λ_{em} of **QC1** and **QC2**) against the mole fraction of Cu^{2+} (Fig. 7a-b) respectively.

DFT studies: The DFT calculations were performed and lowest energy strcutures of the structures of the chemosensors (**QC1** and **QC2**) and the metal complexes of the chemosensors with Cu^{2+} ions (Fig. 8a-b) were developed [37-39]. The difference in the energy-gap between the HOMO and LUMO orbitals was found 3.95 eV and 3.77 eV, respectively, for **QC1** and **QC2**. chemosensors **QC2** with a lower energy gap in HOMO-LUMO orbitals show better reactivity with Cu^{2+} ions [2,3,31]. The complex structure of chemosensors with Cu^{2+} (Fig. 8b) shows the formation of two chealating ring that form a tetrahedral structure with metal ions and in this structure, the fourth valancy was stabilized with used solvent.

Analytical applications: It has been observed that even in the presence of competing metal ions, the compounds **QC1** and **QC2** demonstrate preferential chemosensing capabilities

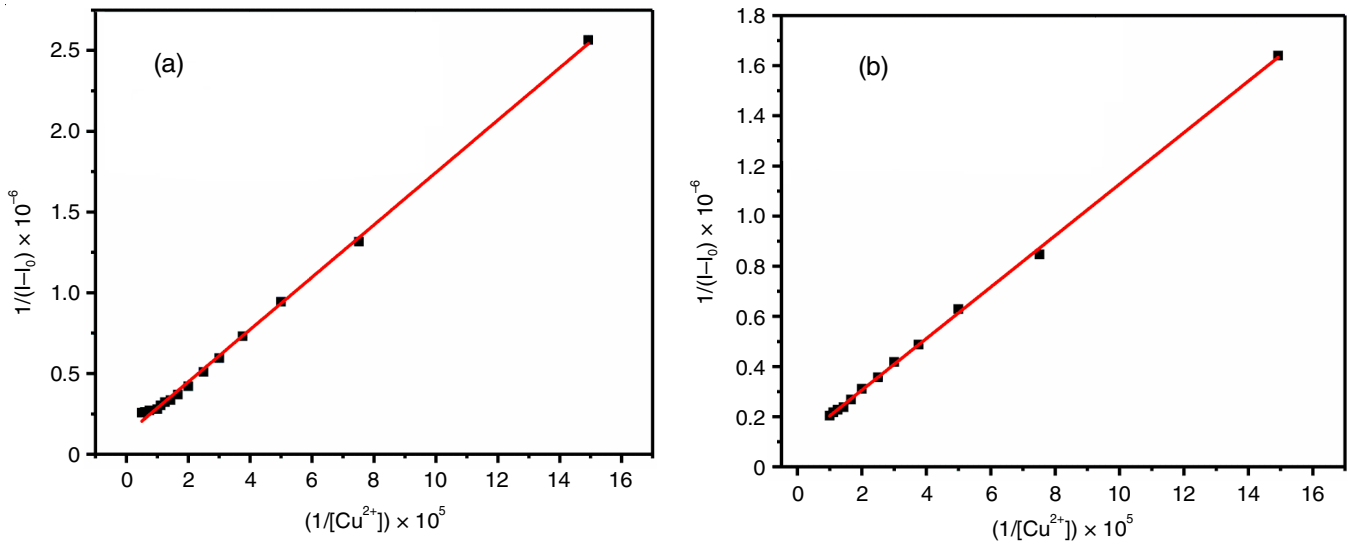

Fig. 4. Binding constant of **QC1** (a) and **QC2** (b) with Cu^{2+} respectively

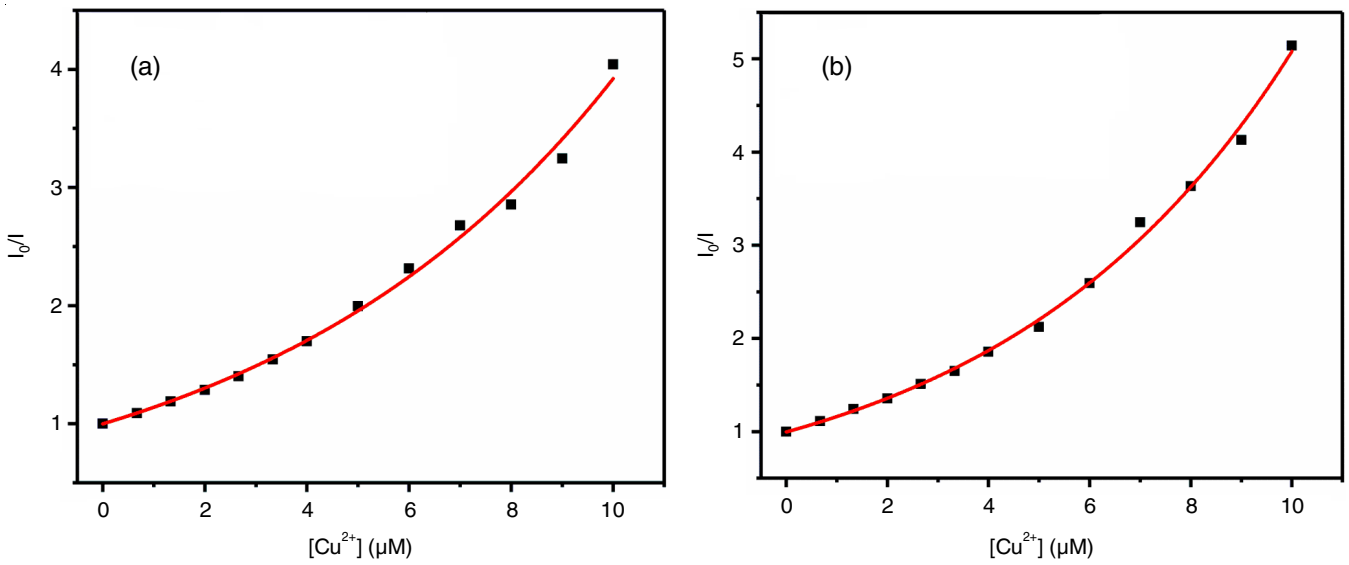

Fig. 5. Stern-Volmer plot of **QC1** (a) and **QC2** (b) with Cu^{2+} respectively

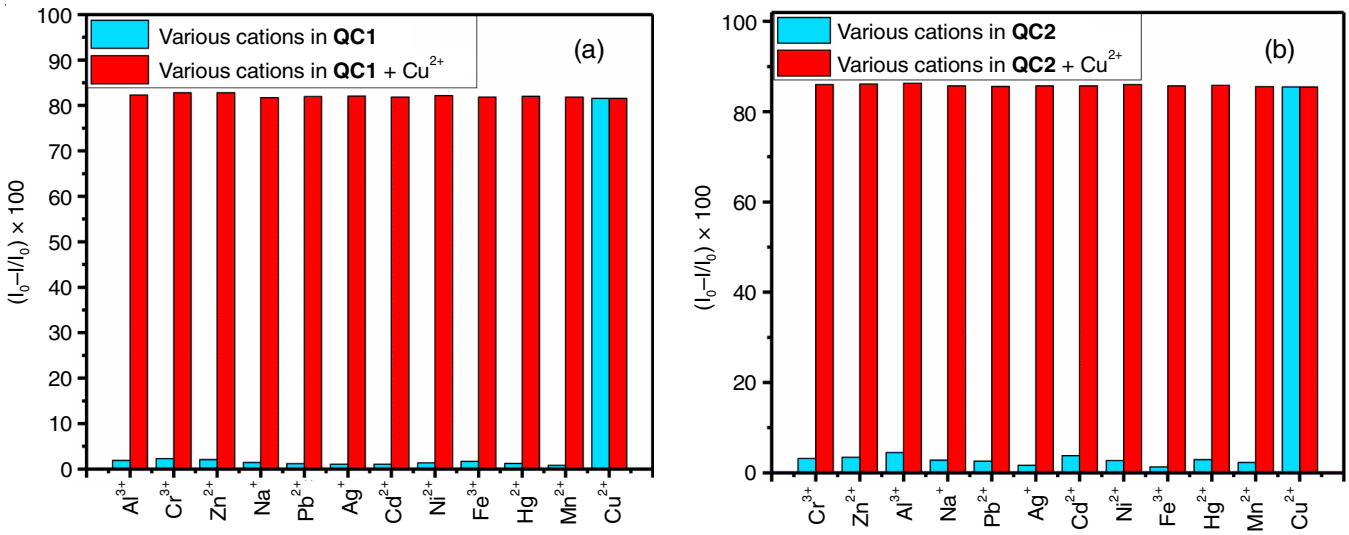

Fig. 6. Fluorescence response of **QC1** (a) and **QC2** (b) (5×10^{-5} M) in MeOH:H_2O (9.5:0.5%,v/v) upon addition of various metal ions (blue bars), followed by addition of 20×10^{-6} M of Cu^{2+} (red bars)

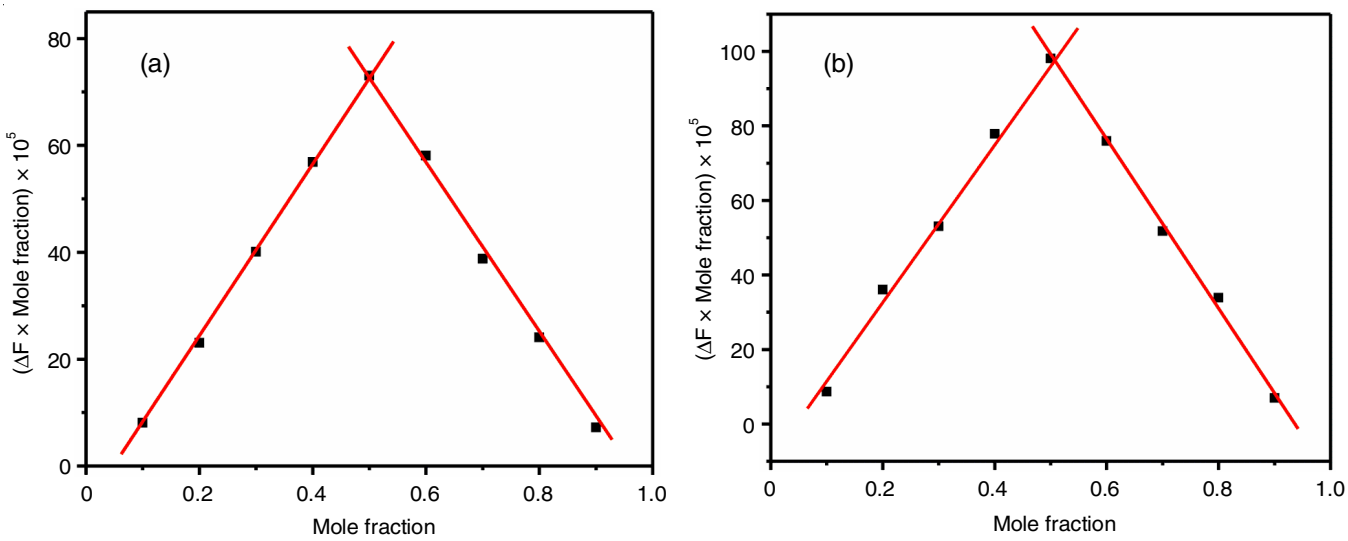

Fig. 7. Job's plot of **QC1** (a) and **QC2** (b) (5×10^{-5} M) towards Cu^{2+}

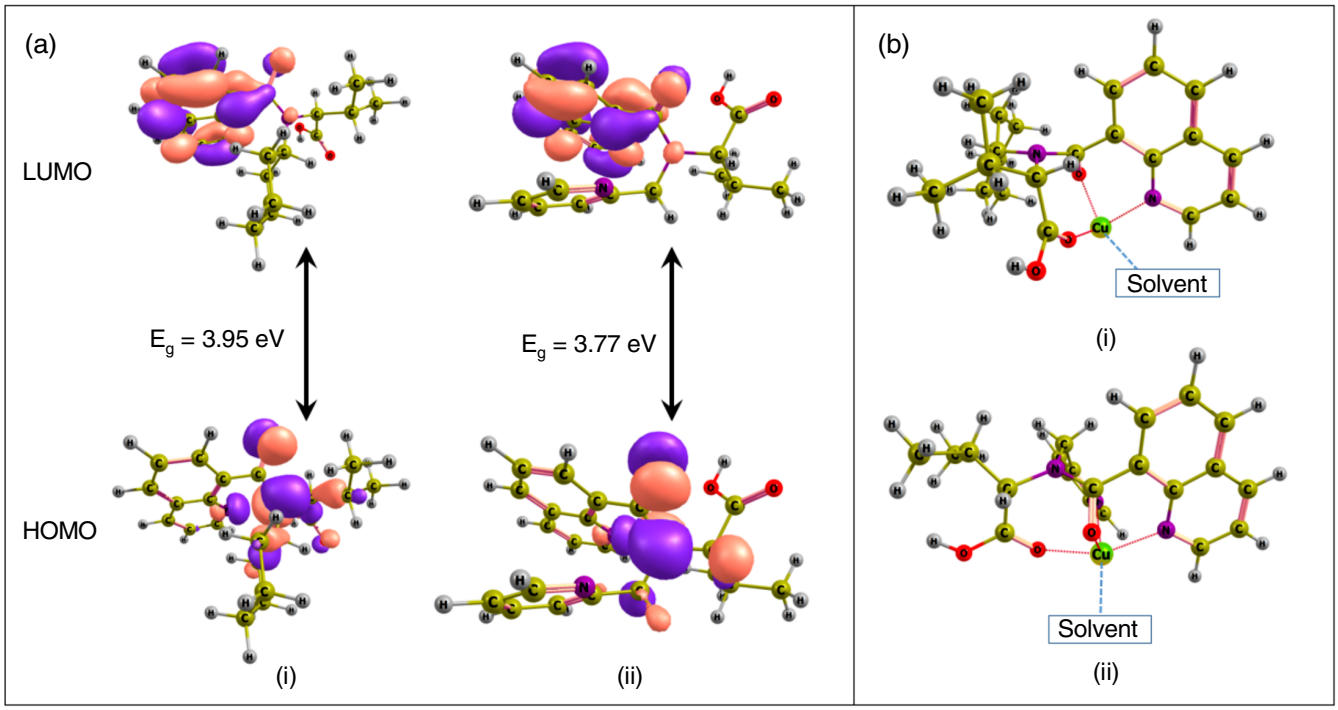

Fig. 8. (a) Geometrically optimized HOMO-LUMO diagrams of (i) **QC1** and (ii) **QC2**; (b) geometrically optimized DFT structures of the metal complexes of (i) **QC1** and (ii) **QC2**

towards Cu^{2+} ions. This observation is significant, therefore, studied the potentialities of **QC1** and **QC2** as chemosensors for analytical uses. However, copper is crucial for many physiological processes and a vital co-factor for many metalloenzymes in living organisms [1-3,40,41]. However, Cu^{2+} is highly hazardous to living things when overloaded. For instance, excessive accumulation in humans results in several illnesses, such as coronary heart disease, metabolic and genetic problems, obesity, diabetes and Wilson's disease [5,6]. The human body can be exposed to Cu^{2+} by heavy metals from soil caused by acid rain or contaminated water from consumer or industrial waste. According to the World Health Organization (WHO), drinking water should contain no more than 2 ppm (30 µg) of copper due to these effects [42,43]. Consequently, developing sensitive and selective fluorescent probes to identify copper in various environment samples is crucial. Hence, we investigated **QC1** and **QC2** chemosensing properties in different environment samples.

Analysis of river water: To achieve this, we generated two sample solutions: sample B, which comprises river water with intentionally added Cu^{2+} (20 µM) ions and sample A, which is river water that has been heated for 5-10 min. **QC2** exhibited a fluorescence emission at 512 nm in MeOH: H_2O (9.5:0.5%, v/v) solution. The fluorescence intensity of **QC2** did not significantly alter when sample A was added to this solution. But when sample B containing Cu^{2+} ions was introduced, **QC2**'s

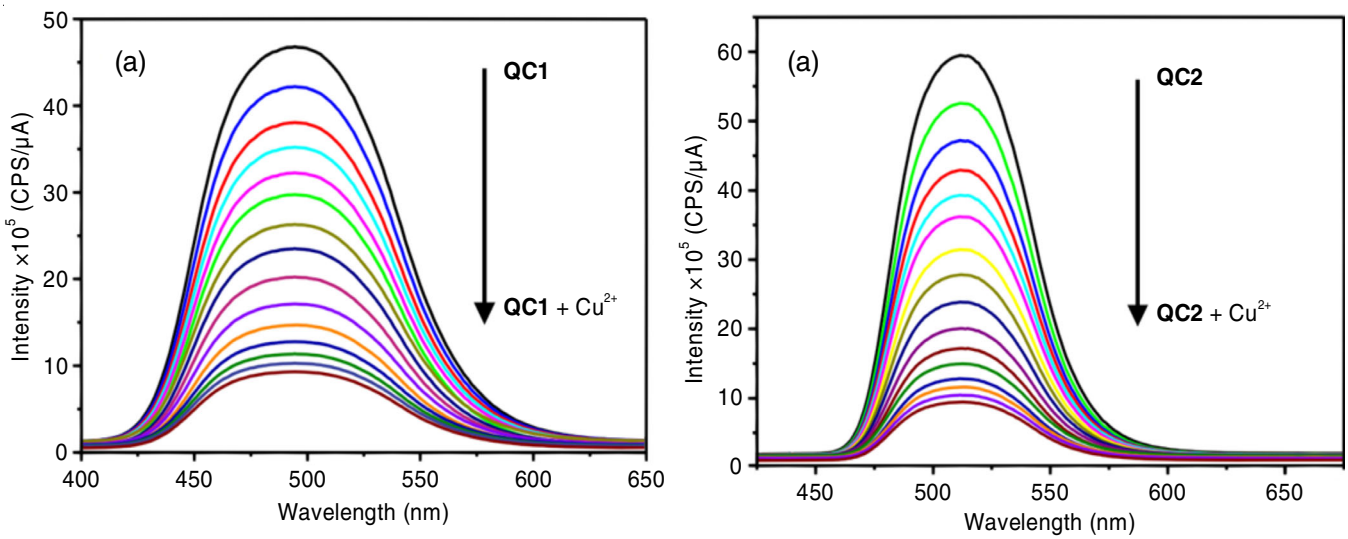

Fig. 9. Fluorescence spectra of **QC1** (a) and **QC2** (b) (5×10^{-5} M) in MeOH:H_2O (river water) (9.5: 0.5%,v/v) upon incremental addition of Cu^{2+} conc.

fluorescence intensity was quenched (Fig. 9a). Compound **QC1** also demonstrated the same outcomes under the same experimental settings, indicating that both compounds have the ability to detect Cu^{2+} in samples of tap water. The limit of detection [35] for **QC1** and **QC2** toward Cu^{2+} in tap water were computed as 55.41 nM and 39.74 nM, respectively. As a result, compared to **QC1** and **QC2** showed the lowest LOD for Cu^{2+} in tap water. In tap water, the binding constants of **QC1** and **QC2** towards Cu^{2+} were calculated as 0.74×10^5 M^{-1} and 1.01×10^4 M^{-1}, respectively. Additionally, the quenching constants towards Cu^{2+} for **QC1** and **QC2** were computed as 1.55×10^5 M^{-1} and 1.07×10^5 M^{-1}, respectively.

Analysis of tap water and industrial waste samples: A similar study was conducted with environmental samples, such as tap water and industrial wastewater. The results were found to be similar to the analysis performed for the river water samples. The spectral hindrance or disturbance was not observed during the fluorescence detection study (similar to Fig. 9). Thus, the developed method is robust and stable even in the presence of unwanted impurities or metal ions.

Conclusion

In summary, a novel class of well-defined chemosensors based on quinoline-based moieties have been developed for as tuneable chemosensors. These chemosensors demonstrated sensitive and specific fluorescence chemosensing capabilities towards Cu^{2+} in nanomolar concentrations. This study indicates that the electronic effects of the substituent can control the photoluminescence and chemosensing properties of this class of compounds. These chemosensors can be used analytically to find traces of Cu^{2+} in industrial waste, river and tap waters. Apart from the chemosensor applications that are the subject of this study, literature studies suggest that these compounds also hold great potential as electron-transport and electroluminescent materials. Analyzing similar chemosensors' characteristics can lead to their development with considerable promise for the aforementioned uses.

ACKNOWLEDGEMENTS

The authors are grateful to the Karnataka State Open University and National Changhua University of Education Taiwan for providing necessary facilities.

CONFLICT OF INTEREST

The authors declare that there is no conflict of interests regarding the publication of this article.

REFERENCES

1. S. Sharma and K.S. Ghosh, *Spectrochim. Acta A Mol. Biomol. Spectrosc.*, **254**, 119610 (2021); https://doi.org/10.1016/j.saa.2021.119610
2. F. Abebe, J. Gonzalez, K. Makins-Dennis and R. Shaw, *Inorg. Chem. Commun.*, **120**, 108154 (2020); https://doi.org/10.1016/j.inoche.2020.108154
3. P. Patil, P.S. Sehlangia, A. Patil, C. Pradeep, S.K. Sahoo and U. Patil, *Spectrochim. Acta A Mol. Biomol. Spectrosc.*, **220**, 117129 (2019); https://doi.org/10.1016/j.saa.2019.05.034
4. S.M. Saleh, R. Ali, F. Alminderej and I.A.I. Ali, *Int. J. Anal. Chem.*, **2019**, Article id 7381046 (2019); https://doi.org/10.1155/2019/7381046
5. N. Chaudhary, P.K. Gupta, S. Eremin and P.R. Solanki, *J. Environ. Chem. Eng.*, **8**, 103720 (2020); https://doi.org/10.1016/j.jece.2020.103720
6. G. Sivaraman, M. Iniya, T. Anand, N.G. Kotla, S. Singaravadivel, O. Sunnapu, A. Gulyani and D. Chellappa, *Coord. Chem. Rev.*, **357**, 50 (2018); https://doi.org/10.1016/j.ccr.2017.11.020
7. S. Liu, Y.M. Wang and J. Han, *J. Photochem. Photobiol. Photochem. Rev.*, **32**, 78 (2017); https://doi.org/10.1016/j.jphotochemrev.2017.06.002
8. J. Liu, Z. Yang, B. Ye, Z. Zhao, Y. Ruan, T. Guo, X. Yu, G. Chen and S. Xu, *J. Mater. Chem. C Mater. Opt. Electron. Devices*, **7**, 4934 (2019); https://doi.org/10.1039/C8TC06292G
9. S. Sehlangia, S. Sharma, S.K. Sharma and C.P. Pradeep, *Mater. Adv.*, **2**, 4643 (2021); https://doi.org/10.1039/D1MA00215E
10. S. Sehlangia, N. Nayak, N. Garg and C.P. Pradeep, *ACS Omega*, **7**, 24838 (2022); https://doi.org/10.1021/acsomega.2c03047

11. B. Li, T. He, X. Shen, D. Tang and S. Yin, *Polym. Chem.*, **10**, 796 (2019); https://doi.org/10.1039/C8PY01396A
12. S. Sehlangia, M. Devi, N. Nayak, N. Garg, A. Dhir and C.P. Pradeep, *ChemistrySelect*, **5**, 5429 (2020); https://doi.org/10.1002/slct.202000674
13. S. Alwera, *ACS Sustain. Chem. Eng.*, **6**, 11653 (2018); https://doi.org/10.1021/acssuschemeng.8b01869
14. S. Alwera and R. Bhushan, *Biomed. Chromatogr.*, **30**, 1223 (2016); https://doi.org/10.1002/bmc.3671
15. M. Albrecht, M. Fiege and O. Osetska, *Coord. Chem. Rev.*, **252**, 812 (2008); https://doi.org/10.1016/j.ccr.2007.06.003
16. C.W. Tang and S.A. VanSlyke, *Appl. Phys. Lett.*, **51**, 913 (1987); https://doi.org/10.1063/1.98799
17. V. Alwera, S. Sehlangia and S. Alwera, *Sep. Sci. Technol.*, **56**, 2278 (2021); https://doi.org/10.1080/01496395.2020.1819826
18. S. Alwera, V. Alwera and S. Sehlangia, *Biomed. Chromatogr.*, **34**, e4943 (2020); https://doi.org/10.1002/bmc.4943
19. S. Alwera and R. Bhushan, *Biomed. Chromatogr.*, **30**, 1772 (2016); https://doi.org/10.1002/bmc.3752
20. V. Alwera, S. Sehlangia and S. Alwera, *J. Liq. Chromatogr. Relat. Technol.*, **43**, 742 (2020); https://doi.org/10.1080/10826076.2020.1798250
21. Raffiunnisa, N. Jaishetty, P. Ganesh, M.S. Patel, V.S. Talismanov, S. Alwera and S. Sehlangia, *Asian J. Chem.*, **35**, 1855 (2023); https://doi.org/10.14233/ajchem.2023.28037
22. M. Schaefer, N. Hanik and A.F.M. Kilbinger, *Macromolecules*, **45**, 6807 (2012); https://doi.org/10.1021/ma301061z
23. E.C. Davison, I.T. Forbes, A.B. Holmes and J.A. Warner, *Tetrahedron*, **52**, 11601 (1996); https://doi.org/10.1016/0040-4020(96)00643-6
24. A. Edwards and M. Rubin, *Org. Biomol. Chem.*, **14**, 2883 (2016); https://doi.org/10.1039/C6OB00156D
25. L. Zhang, X.J. Wang, J. Wang, N. Grinberg, D.K. Krishnamurthy and C.H. Senanayake, *Tetrahedron Lett.*, **50**, 2964 (2009); https://doi.org/10.1016/j.tetlet.2009.03.220
26. S. Alwera and R. Bhushan, *J. Liq. Chromatogr. Relat. Technol.*, **40**, 707 (2017); https://doi.org/10.1080/10826076.2017.1348954
27. S. Alwera and R. Bhushan, *Biomed. Chromatogr.*, **31**, e3983 (2017); https://doi.org/10.1002/bmc.3983
28. V. Alwera, S. Sehlangia and S. Alwera, *Biomed. Chromatogr.*, **34**, e4954 (2020); https://doi.org/10.1002/bmc.4954
29. H.S. Al-Shehri, V. Alwera, K.C. Nilugal and S. Alwera, *Asian J. Chem.*, **34**, 376 (2022); https://doi.org/10.14233/ajchem.2022.23550
30. D.J. Hardee, L. Kovalchuke and T.H. Lambert, *J. Am. Chem. Soc.*, **132**, 5002 (2010); https://doi.org/10.1021/ja101292a
31. G. Yuan, G. Hu, W. Shan, S. Jin, Q. Gu and J. Chen, *Dalton Trans.*, **44**, 17774 (2015); https://doi.org/10.1039/C5DT02692J
32. Y. Huo, J. Lu, S. Hu, L. Zhang, F. Zhao, H. Huang, B. Huang and L. Zhang, *J. Mol. Struct.*, **1083**, 144 (2015); https://doi.org/10.1016/j.molstruc.2014.11.029
33. J. Bell, I. Samb, P.Y. Toullec, O. Mongin, M. Blanchard-Desce, V. Michelet and I. Leray, *New J. Chem.*, **38**, 1072 (2014); https://doi.org/10.1039/C3NJ01308A
34. G.L. Long, E.G. Voigtman, M.A. Kosinski and J.D. Winefordner, *Anal. Chem.*, **55**, 1432 (1983); https://doi.org/10.1021/ac00259a060
35. M. Devi, A. Dhir and C.P. Pradeep, *New J. Chem.*, **40**, 1269 (2016); https://doi.org/10.1039/C5NJ02175H
36. P. Job, *Ann. Chim.*, **9**, 113 (1928).
37. T.I. Ahmed, V. Alwera, V.S. Talismanov, N. Jaishetty, S. Sehlangia and S. Alwera, *Asian J. Chem.*, **34**, 1213 (2022); https://doi.org/10.14233/ajchem.2022.23706
38. H.S. Al-Shehri, M.S. Patel, S. Alwera, V.S. Talismanov, V. Alwera and R.R. Macadangdang Jr, *Asian J. Chem.*, **34**, 673 (2022); https://doi.org/10.14233/ajchem.2022.23578
39. M. Solanki, S. Sehlangia, V.S. Talismanov, A. Damayanthi, M.S. Patel, S. Shrivastava and S. Alwera, *Asian J. Chem.*, **36**, 404 (2024); https://doi.org/10.14233/ajchem.2024.30926
40. B. Kaur, N. Kaur and S. Kumar, *Coord. Chem. Rev.*, **358**, 13 (2018); https://doi.org/10.1016/j.ccr.2017.12.002
41. M. Rajasekar, S. Geetha Sree Agash, C. Narendran and K. Rajasekar, *Inorg. Chem. Commun.*, **151**, 110609 (2023); https://doi.org/10.1016/j.inoche.2023.110609
42. A. Ramdass, V. Sathish, E. Babu, M. Velayudham, P. Thanasekaran and S. Rajagopal, *Coord. Chem. Rev.*, **343**, 278 (2017); https://doi.org/10.1016/j.ccr.2017.06.002
43. T. Chopra, S. Sasan, L. Devi, R. Parkesh and K.K. Kapoor, *Coord. Chem. Rev.*, **470**, 214704 (2022); https://doi.org/10.1016/j.ccr.2022.214704